Radical Anion Complexes of Tris(1,3-diphenyltriazenido)aluminum

Janet Braddock-Wilking, John T. Leman, Christian T. Farrar, Sarah A. Cosgrove-Larsen, David J. Singel, and Andrew R. Barron

J. Am. Chem. Soc., **1995**, 117 (6), 1736-1745 • DOI: 10.1021/ja00111a010

Radical Anion Complexes of Tris(1,3-diphenyltriazenido)aluminum

Janet Braddock-Wilking, John T. Leman, Christian T. Farrar, Sarah C. Larsen, David J. Singel,*,† and Andrew R. Barron*

Contribution from the Department of Chemistry, Harvard University, Cambridge, Massachusetts 02138

Received February 22, 1994[⊗]

Abstract: Electrochemical studies of $Al(dpt)_3$ (Hdpt = 1,3-diphenyltriazene) by cyclic voltammetry in THF solution reveal three successive pseudo reversible one-electron reduction waves ($E_{1/2}$ = −1.50, −1.84, and −2.16 V). The chemical reduction of $Al(dpt)_3$ by sodium metal in THF allows for the isolation of the radical anion complexes $[Na(THF)_x]_n[Al(dpt)_3]$, n = 1 (**1**), 1 (**2**), and 3 (**3**). Characterization by EPR, NMR, UV−visible, and X-ray photoelectron (XP) spectroscopy, in addition to the X-ray structural determination of $[PPN][Al(dpt)_3]$ (**4**), supports the formation of the first homologous series of ligand-centered aluminum(III) radical anion complexes. Analogous electrochemical reduction series are observed for the *p*-methyl- and *p*-methoxy-substituted triazenides. The dependence of the complex reduction potentials is discussed with respect to the UV−visible spectra of the unreduced complex and the ligand's Hammett substituent constant (σ). In contrast, irreversible electrochemical reduction (−1.5 to −2.2 V) occurs for the pentafluoro- and *p*-fluoro-, *p*-chloro-, and *p*-bromo-substituted triazenido complexes. Irreversible reduction also occurs for the alkyl and aryloxide compounds $Al(R)_2(dpt)$ (R = ^{i}Bu, ^{t}Bu), $Al(^i Bu)(dpt)_2$, $Al(BHT)_2(dpt)$, and $Al(BHT)(dpt)_2$ (BHT−H = 2,6-di-*tert*-butyl-4-methylphenol). *Ab initio* molecular orbital calculations have been carried out on the model compounds $Al(HNNNH)_3$ and $[Al(HNNNH)_3]^{3-}$. The identity of the frontier molecular orbitals and calculated structures are considered in relation to experimental data.

Introduction

Over the last 30 years, a number of compounds have been reported that would appear to contain aluminum in the formal oxidation states of 0, +1, or +2. In most cases, low valency was proposed on the basis of the paramagnetic nature of the compounds, but in each instance, detailed spectroscopic characterization has subsequently indicated otherwise.[1] It is, of course, a consequence of the $[Ne]3s^03p^0$ configuration of Al^{3+} that the vast majority of aluminum compounds are trivalent and diamagnetic. It is only within the last few years that low-valent compounds of aluminum have been isolated and crystallographically characterized.[1] However, interest in paramagnetic aluminum compounds has continued because of mechanistic studies on the reactions of coordinated ligands, in particular organic carbonyls, which have often been proposed to proceed *via* the formation of ligand-centered radical intermediates.[2]

The first report of an isolated compound with an apparently low-valent aluminum center was that of the neutral complex $Al(bipy)_3$ (bipy = 2,2′-bipyridyl).[3] Subsequent magnetic measurements[4] showed that, although $Al(bipy)_3$ is paramagnetic, it can best be explained by postulating an Al^{3+} cation, with the unpaired electrons extensively delocalized on the ligands, giving rise to three bipy radical anions. Further evidence for this picture was gained by investigations of the intermolecular interactions of $Al(bipy)_3$ with tetracyanoethylene.[5]

Following the work with $Al(bipy)_3$, a wide range of related organoaluminum radicals, $[R_2Al(L)]^{\bullet}$, were isolated.[1] In each case, the aluminum is in the formal oxidation state of +2. However, EPR measurements and HMO calculations indicated that all of these compounds are best considered as being complexes of the dialkylaluminum cations, $[R_2Al]^+$, with the radical anions of the pyridine, pyrazine, or bipyridine ligands.[6] Recent efforts, by Raston and co-workers,[7] to prepare low-valent aluminum complexes have concentrated on the reaction of 1,4-di-*tert*-butyl-1,4-diazabutadiene (dbdab) with either aluminum metal or alanes. However, EPR and photoelectron spectroscopy[8] suggest that in the products $Al(dbdab)_2$ and $Al(dbdab)[N(^tBu)CH_2]_2$, the unpaired electron is primarily ligand-centered with the aluminum in a trivalent state.[9]

Despite the proposal[8] that $Al(dbdab)_2$ should be readily oxidized to give the cation, $[Al(dbdab)_2]^+$, where both ligands are singly reduced, no attempt has been made to prepare a homologous series from a neutral complex to either the trication (eq 1) or trianion (eq 2).

* Authors to whom correspondence should be addressed.

† Current address: Department of Chemistry, Montana State University, Bozeman, MT 59717.

⊗ Abstract published in *Advance ACS Abstracts,* January 15, 1995.

(1) For a recent review of low-valent and paramagnetic compounds of aluminum, see: Barron, A. R. In *Coordination Chemistry of Aluminum*; Robinson, G. H., Ed.; VCH: New York, 1993; Chapter 4, p 123.

(2) See, for example: (a) Boone, J. R.; Ashby, E. C. *Top. Stereochem.* **1979**, *11*, 53. (b) Haubenstock, H. *Top. Stereochem.* **1983**, *14*, 231. (c) Noth, H. *Z. Naturforsch B* **1980**, *35*, 119. (d) Ashby, E. C.; DePriest, R. N.; Pham, T. N. *Tetrahedron Lett.* **1983**, *24*, 2825. (e) Power, M. B.; Bott, S. G.; Atwood, J. L.; Barron, A. R. *J. Am. Chem. Soc.* **1990**, *112*, 2446.

(3) Herzog, S.; Geisler, K.; Präkel, H. *Angew. Chem., Int. Ed. Engl.* **1963**, *2*, 47.

(4) Ionue, M.; Horiba, T.; Hara, K. *Bull. Chem. Soc. Jpn.* **1978**, *51*, 3073.

(5) Flamini, A.; Poli, N. *Inorg. Chim. Acta* **1988**, *150*, 149.

(6) (a) Köster, R.; Benedikt, G.; Schrötter, H. W. *Angew. Chem., Int. Ed. Engl.* **1964**, *3*, 514. (b) Lehmkuhl, H.; Fuchs, G.; Köster, R. *Tetrahedron Lett.* **1965**, 29, 2511. (c) Kaim, W. *J. Organomet. Chem.* **1980**, *201*, C5. (d) Kaim, W. *Chem. Ber.* **1981**, *114*, 3789. (e) Kaim, W. *Z. Naturforsh.* **1982**, *37B*, 783.

(7) Cloke, F. G. N.; Dalby, C. I.; Henderson, M. J.; Hitchcock, P. B.; Kennard, C. H. L.; Lamb, R. N.; Raston, C. L. *J. Chem. Soc., Chem. Commun.* **1990**, 1394.

(8) Cloke, F. G. N.; Dalby, C. I.; Daff, P. J.; Green, J. C. *J. Chem. Soc., Dalton Trans.* **1991**, 181.

(9) It is worth noting that while the aluminum compounds were proposed to be Al(III), the gallium analogue was proposed to be Ga(II). This was subsequently disproved: Kaim, W.; Matheis, W. *J. Chem. Soc., Chem. Commun.* **1991**, 597.

0002-7863/95/1517-1736$09.00/0

$$AlL_x \xrightarrow{-e^-} [AlL_x]^+ \xrightarrow{-e^-} [AlL_x]^{2+} \xrightarrow{-e^-} [AlL_x]^{3+} \quad (1)$$

$$AlL_x \xrightarrow{+e^-} [AlL_x]^- \xrightarrow{+e^-} [AlL_x]^{2-} \xrightarrow{+e^-} [AlL_x]^{3-} \quad (2)$$

In a previous publication,[10] we have described the preparation and characterization of the tris(1,3-diphenyltriazenido) complexes of aluminum, gallium, and indium, $M(dpt)_3$ (**I**), from 1,3-diphenyltriazene (Hdpt) and the appropriate group 13 trimethyl (eq 3). Since the 1,3-diphenyltriazenide ligand has

$$MMe_3 + 3Hdpt \xrightarrow[M = Al, Ga, In]{} M(dpt)_3 + 3MeH \quad (3)$$

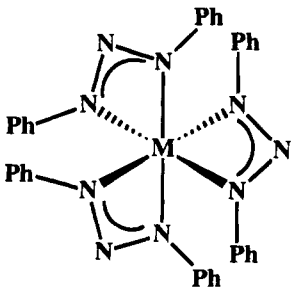

M = Al, Ga, In

(**I**)

been shown to be resistant to fragmentation,[11] and is found to stabilize a number of paramagnetic transition metal complexes,[12] we undertook an investigation of the formation of a series of anionic radical complexes based on the aluminum triazenide, *i.e.*, $[Al(dpt)_3]^{n-}$ (n = 1, 2, and 3). The results of this study are described herein.

Results and Discussion

Electrochemistry of Al(dpt)$_3$. Electrochemical studies of $Al(dpt)_3$ by cyclic voltammetry (CV) at room temperature in THF solution reveal three successive reduction waves (−1.50, −1.84, and −2.16 V) with nearly identical interwave spacing (320−340 mV) (see Figure 1 and Table 1). These redox processes are quasi reversible, with peak-to-peak separations exceeding the Nernstian value of 57 mV, though this broadening may be partially attributed to resistance effects,[13] which are appreciable in THF solution.[14] The relative magnitude of peak cathodic and anodic currents is perhaps more diagnostic of the reversibility of a redox process, but its determination is not without complications in this instance. Since the current base line for each succeeding wave is superimposed on the decaying current peak for the previous one, the ratio I_{p_a}/I_{p_c} cannot be determined with absolute certainty.[15] Qualitatively, this circumstance gives the appearance of unequal peak currents for each reduction. For $Al(dpt)_3$, the estimated (see ref 15) values of the parameter I_{p_a}/I_{p_c} for each voltammetric wave (0.86−0.89) indicate a system with some limited degree of chemical reversibility. This irreversibility becomes more pronounced at scan rates less than 100 mV s^{-1}. Consequently, the measurement of the number of electrons transferred to each redox process by controlled potential electrolysis was not successful. However, a differential pulsed polarogram (DPP) of $Al(dpt)_3$ (Figure 2), in which the peak heights are directly proportional to the concentration of electroactive species, clearly shows the equivalence of peak cathodic currents and indicates that the three reduction waves involve the transfer of equal quantities of reducing equivalents.[16]

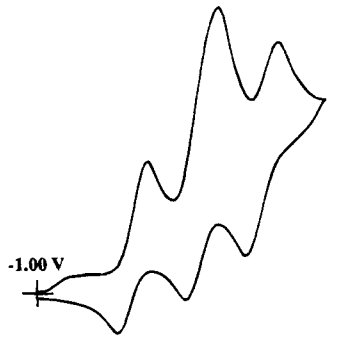

Figure 1. Cyclic voltammogram of $Al(dpt)_3$ in THF with 0.1 M $[^nBu_4N][PF_6]$ as supporting electrolyte, ferrocene as an external reference (0.55 V), and a sweep rate of 100 mV s^{-1}. $E^1_{1/2} = -1.50$ V, $\Delta E^1_p = 130$ mV; $E^2_{1/2} = -1.84$ V, $\Delta E^2_p = 120$ mV; and $E^3_{1/2} = -2.16$ V, $\Delta E^3_p = 140$ mV.

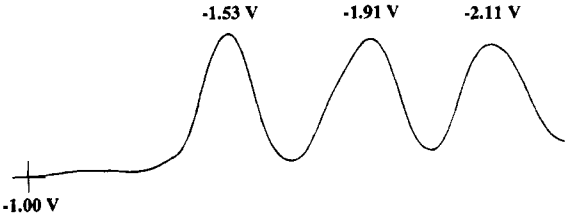

Figure 2. Differential pulsed polarogram of $Al(dpt)_3$ in THF. Relative peak heights (scaled to the first reduction wave), 1.00, 0.96, and 0.92. Pulse width, 57 ms; pulse amplitude, 50 mV; sweep rate, 50 mV s^{-1}.

While it is tempting to invoke a sequential, three-electron, metal-centered process involving the reduction of the aluminum center to the formal oxidation states +2, +1, and 0, it has generally been observed that the number of redox waves for homoleptic chelating complexes equals the number of chelating ligands.[17] Therefore, in the absence of further information, it is equally tenable to propose that this result is due to the formation of a series of radical anion species formed by successive reduction of each of the triazenide ligands (*cf.* eq 2). The viability of this proposal is explored through the chemical synthesis, isolation, and complete characterization of the reduced $Al(dpt)_3$ species given below.

Radical Anions of Al(dpt)$_3$: Synthesis and Spectroscopic Characterization. The stoichiometric reduction of $Al(dpt)_3$ with sodium metal[18] in THF affords the corresponding radical anion complexes $[Na(THF)_x]_n[Al(dpt)_3]$ ($x \approx 4$,[19] n = 1, 2, and 3), according to eq 4. The monoreduced species may also be isolated as the PPN [bis(triphenylphosphine)iminium] salt *via*

$$Al(dpt)_3 + n\text{Na} \xrightarrow[THF]{} [Na(THF)_x]_n[Al(dpt)_3] \quad n = 1\ (\mathbf{1}),\ 2\ (\mathbf{2}),\ 3\ (\mathbf{3}) \quad (4)$$

Table 1. Electrochemical Data for Aluminum Triazenide Compounds

	E^1			E^2			E^3		
compound	$E_{1/2}$ (V)[a]	ΔE_p (mV)	(I_{p_a}/I_{p_c})	$E_{1/2}$ (V)[a]	ΔE_p (mV)	(I_{p_a}/I_{p_c})	$E_{1/2}$ (V)[a]	ΔE_p (mV)	(I_{p_a}/I_{p_c})
$Al(dpt)_3$	−1.50	130	0.89	−1.84	120	0.86	−2.16	120	0.89
$Al(dpt\text{-}4\text{-}Me)_3$[b]	−1.64	210	0.88	−2.00	230	0.98	−2.37	180	0.87
$Al(dpt\text{-}4\text{-}OMe)_3$[b]	−1.72	130	0.96	−2.10	140	0.71	−2.46	190	0.63
$Al(dpt^*)_3$[b,c]	−1.63	180	0.83	−2.00	230	0.92	−2.38	250	1.0

[a] $E_{1/2} = (E_{p_a} + E_{p_c})/2$; $\Delta E_p = (E_{p_a} - E_{p_c})$. [b] dpt-4-X = 1,3-bis(4-X-phenyl)triazenide. [c] dpt* = 1-(*p*-methoxyphenyl)-3-phenyltriazenide.

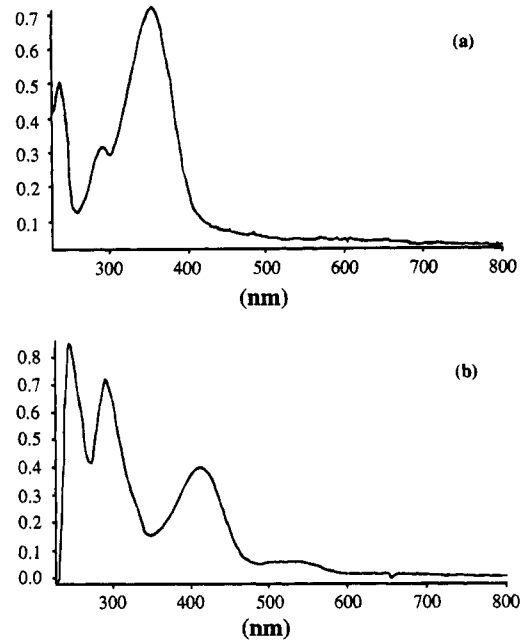

Figure 3. UV−visible spectra of THF solutions of (a) $Al(dpt)_3$ and (b) $[Na(THF)_4]_3[Al(dpt)_3]$.

the metathesis reaction given in eq 5 (see Experimental Section).

$$[Na(THF)_x][Al(dpt)_3] + [PPN]Cl \rightarrow [PPN][Al(dpt)_3] + NaCl \quad (5)$$
$$(4)$$

The complexes (**1**−**4**) are isolated as dark purple-black solids that are stable at room temperature under an inert atmosphere, both in solution and in the solid state, although they react rapidly with atmospheric water and oxygen. In the case of compound **3**, the reaction is sufficiently violent to cause combustion of solid samples. However, reoxidation with oxygen at −78 °C allows for the recovery of $Al(dpt)_3$ (see Experimental Section). While there is little conductivity data available for species in THF solution, the values for **1**, **2**, and **3** in THF (see Experimental Section) are indicative of ionic species, *i.e.*, THF solutions of **1**, **2**, and **3** have molar conductivities comparable to, or greater than, that of $[^nBu_4N][PF_6]$ and at least 12 times greater than that of the neutral $Al(dpt)_3$ in the same solvent.[20] These results are in accord with the ionic formulation of **1**, **2**, and **3**.

The UV−visible spectrum for $Al(dpt)_3$ (Figure 3a) shows three principal absorption bands at 354 (ϵ = 65 000 L mol^{-1} cm^{-1}), 294 (ϵ = 29 000 L mol^{-1} cm^{-1}), and 238 (ϵ = 46 000 L mol^{-1} cm^{-1}) nm. The latter two bands appear at wavelengths comparable to those observed in aniline and are characteristic of aromatic amines in general.[21] By analogy to the lowest energy band of the uncomplexed ligand (350 nm), the band at 354 nm (ϵ = 65 000) for $Al(dpt)_3$ is attributable to the $\pi \rightarrow \pi^*$ transition for the triazenide's unsaturated N_3 framework.[22,23] As can be seen from Figure 3b, upon reduction with 3 equiv of sodium, *i.e.*, compound **3**, the band at 354 nm is bathochromically shifted to lower energy (412 nm). In addition, a new band is observed (520 nm, ϵ = 5500), which we tentatively assign to a charge-transfer transition from the singly occupied π^* orbital of the reduced triazenide's N_3 unit (see below) to the π^* orbital of the adjacent phenyl rings. The bands at 294 and 238 nm are essentially unchanged upon ligand reduction. The spectra for compounds **1** and **2** contain broad overlapping absorption bands characteristic of both unreduced and reduced triazenide ligands. The relative intensities of these bands (unreduced *vs* reduced) change in a manner consistent with the stepwise reduction of one, two, and three triazenide ligands, *i.e.*, the bands at 412 and 520 nm increase in intensity at the expense of the band at 354 nm (see Experimental Section). There is no difference in the spectrum of **1** and the PPN salt (see below). These spectra are, therefore, consistent with the successive and independent reduction of each of the triazenide ligands (eq 6).

$$Al(dpt)_3 \xrightarrow{+e^-} [Al(dpt)_2(dpt^\bullet)]^- \xrightarrow{+e^-} [Al(dpt)(dpt^\bullet)_2]^{2-} \xrightarrow{+e^-} [Al(dpt^\bullet)_3]^{3-} \quad (6)$$

Further evidence for the ligand-centered nature of the redox process may be obtained from a comparison of the ^1H and ^{27}Al NMR spectra of $Al(dpt)_3$ and $[PPN][Al(dpt)_3]$. The ^{27}Al NMR spectrum of $Al(dpt)_3$ consists of a broad peak ($W_{1/2}$ = 1160 Hz) whose shift (δ = 25) is indicative of a six-coordinate aluminum center. Upon reduction, the resonance moves slightly downfield (δ = 56) but increases dramatically in line width, $W_{1/2}$ = 7500 Hz (see Figure 4). The increased line width of the reduced species as compared to the neutral complex is undoubtedly due to the paramagnetic nature of the reduced complex.[24] If the unpaired electron were located primarily on the aluminum, no signal should be observed due to overwhelming paramagnetic line broadening. Conversely, if the unpaired electron is primarily ligand-centered, then moderate line broadening should be observed. In addition, a contact shift, $\Delta\delta$ (eq

(10) Leman, J. T.; Barron, A. R.; Ziller, J. W.; Kren, R. M. *Polyhedron* **1989**, *8*, 1909.

(11) Moore, D. S.; Robinson, S. D. *Adv. Inorg. Chem. Radiochem.* **1986**, *30*, 1.

(12) (a) Pfeiffer, E.; Kokkes, M. W.; Vrieze, K. *Transition Met. Chem.* **1979**, *4*, 393. (b) Vanderlinden, J. G. M.; Dix, A. H.; Pfeiffer, E. *Inorg. Chim. Acta* **1980**, *39*, 271. (c) Connelly, N. G.; Finn, C. J.; Freeman, M. J.; Orpen, A. G.; Stirling, J. *J. Chem. Soc., Chem. Commun.* **1984**, 1025.

(13) Sawyer, D. T.; Roberts, J. L. *Experimental Electrochemistry for Chemists*; Wiley: New York, 1974; p 188.

(14) ΔE_p values even for highly reversible couples often exceed the theoretical value in solvents of low dielectric constant, especially THF. See, for example: (a) Gagne, R. C.; Koval, C. A.; Lisensky, G. C. *Inorg. Chem.* **1980**, *19*, 2855. (b) Brisdon, B. J.; Conner, K. A.; Walton, R. A. *Organometallics* **1983**, *2*, 1159. (c) Santure, D. J.; Huffman, J. C.; Sattelberger, A. P. *Inorg. Chem.* **1985**, *24*, 371. (d) Zeitlow, T. C.; Klendworth, D. D.; Nimry, T.; Salmon, D. J.; Walton, R. A. *Inorg. Chem.* **1985**, *24*, 947.

(15) The problem of measuring base-line currents for multiple, closely spaced reduction waves has been discussed by Bard and others: (a) Bard, A. J.; Faulkner, L. R. *Electrochemical Methods*; Wiley: New York, 1980; p 232. (b) Geiger, W. E. In *Inorganic Reactions and Methods*; Zuckerman, J. J., Ed.; VCH: Deerfield Beach, FL, 1986; Vol. 15, p 123.

(16) We note that a slight hump is observed on the second reduction wave in the DPP (see Figure 2), as a consequence of either (a) the mildly irreversible nature of the reduction waves resulting in the formation of an electrochemically active decomposition product or (b) the presence of an "adsorption peak", *i.e.*, observation of a distinct species absorbed onto the surface of an electrode rather than at the solid−liquid interface.

(17) Morris, D. E.; Hanck, K. W.; DeArmond, M. K. *J. Electroanal. Chem. Interfacial Electrochem.* **1983**, *149*, 115.

(18) The reduction of $Al(dpt)_3$ may also be accomplished with Li metal, Na/Hg amalgam, and sodium naphthalenide (see Experimental Section).

(19) The extreme sensitivity of these radical compounds and the lability of the THF preclude the exact determination of the number of coordinated solvent molecules by elemental analysis. However, an approximate value of four per sodium cation may be determined by ^1H NMR spectroscopy. This is consistent with literature data: Cotton, F. A.; Wilkinson, G. *Advanced Inorganic Chemistry*; Wiley: New York, 1988; p 133.

(20) Molar conductivities in THF solution (≈1 mM) are $[^nBu_4N][PF_6]$ (Λ_M = 7.2 Ω^{-1} cm^2 mol^{-1}) and $Al(dpt)_3$ (Λ_M = 0.53 Ω^{-1} cm^2 mol^{-1}).

(21) Day, B. F.; Campbell, T. W.; Coppinger, G. M. *J. Am. Chem. Soc.* **1951**, *73*, 4687.

(22) Rukhadze, E. G.; Ershova, T. V.; Fedorova, S. A.; Terent'ev, A. P. *Russ. J. Inorg. Chem.* **1969**, *39*, 283.

(23) Zaitseu, B. E.; Zaitseva, V. A.; Molodkin, A. K.; Lisitsina, E. S. *Russ. J. Inorg. Chem.* **1977**, *22*, 504.

(24) Eaton, D. R.; Philips, W. D. *Adv. Magn. Reson.* **1965**, *1*, 103.

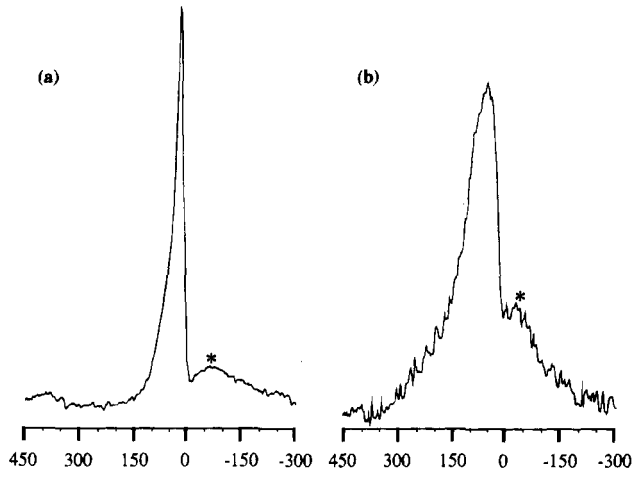

Figure 4. ^{27}Al NMR spectra of (a) Al(dpt)$_3$ and (b) [Al(dpt)$_3$]$^-$. Features labeled with an asterisk (*) are due to the spectrometer probe.

7), of the aluminum nucleus should be induced by delocalization

$$\Delta\delta = \delta_{Al(dpt)_3} - \delta_{[Al(dpt)_3]^{n-}} \quad (7)$$

of the unpaired electrons from the ligand to the metal. The magnitude of the contact shift will be dependent on the extent of interaction between the observed nucleus and the unpaired spin. In the present case, while we have no examples for direct comparison, the small contact shift observed ($\Delta\delta$ = 31 ppm) suggests a limited interaction between the aluminum center and the unpaired electron; *i.e.*, the radical is ligand-centered.

As may be expected, the ^{1}H NMR resonances for each of the compounds are uniformly shifted to a higher field with respect to Al(dpt)$_3$ in the same solvent.[25] Since the magnitude of this contact shift is small ($\Delta\delta$ = 0.13−0.40 ppm), the interaction between unpaired spins and the aromatic protons must be minimal, consistent with the absence of ^{1}H hyperfine splitting in the EPR spectra (see below). The lack of variation in chemical shift between compounds **1**−**3** is consistent with the relative independence of the aromatic rings and paramagnetic centers (see below). However, we note that, since the isotropic shifts may be due to a combination of dipolar and contact components,[26] no definitive conclusion can be reached.

The frozen solution EPR spectra (77 K) of reduced complexes **1**−**4** are all similar in that they contain relatively featureless resonances consisting of two unresolved shoulders symmetrically placed about a broad central line (*e.g.*, Figure 5a). In the case of the PPN salt **4**, shown in Figure 5b, slightly better resolution is seen, perhaps attributable to more effective magnetic dilution as a result of increased cation−anion segregation in the frozen matrix (see below). Even so, it would appear that little quantitative information may be gleaned from these spectra, but we note several qualitative aspects that provide some additional knowledge of these spin systems. The g value for all four compounds is similar (g_{av} = 2.0163 ± 0.0010) and is appropriate for an organic radical. No transitions are observed at the lower field for the doubly and triply reduced species **2** and **3**, and the spectra for both appear isotropic with no apparent dipolar coupling between radical centers. The line shape and lack of interaction between radical centers are reminiscent of [Ru(bipy)$_3$]^n (n = 1, 0, and −1) compounds, which contain

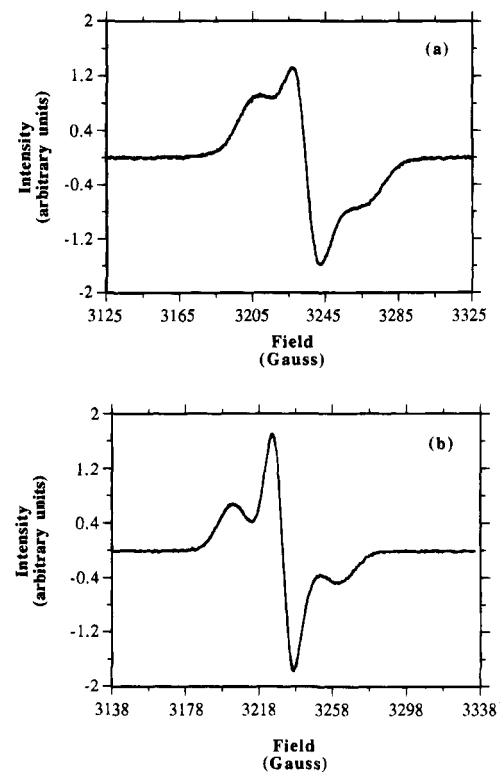

Figure 5. EPR spectra of (a) [Na(THF)$_4$][Al(dpt)$_3$] (**1**) and (b) [PPN][Al(dpt)$_3$] (**4**) in frozen THF (77 K).

independent anion radical bipy ligands and function as essentially isolated S = $^1/_2$ centers.[27]

Of more importance to the specific nature of the radical species, no hyperfine coupling is discernible for an I = $^5/_2$ nucleus (^{27}Al) as would be seen in a metal-centered radical such as [AlH$_3$]$^-$.[28] In addition, the absence of ^{1}H hyperfine structure argues against the electron spin being localized on a phenyl ring. This observation is in accord with the small contact shifts seen in both the ^{27}Al and ^{1}H NMR spectra. The triplet-like structure of these spectra is more suggestive of primary coupling to a single ^{14}N center. However, such a coupling would be expected to produce a 1:1:1 triplet in fluid solution, which is not observed, indicating that a more complex description for the spin system is necessary. In this regard, we have undertaken a detailed EPR−ESEEM study to fully elucidate the details of the electronic structure of these molecules.[29] Irrespective of these complications, the frozen solution EPR spectra clearly confirm the presence of a series of ligand-centered radicals in which the unpaired electron density resides on the ligands' N$_3$ unit.

The localization of the unpaired electron(s) on the N$_3$ centers of the triazene ligand(s) in [Al(dpt)$_3$]$^{n-}$ should result in the reduction of the formal oxidation state of the nitrogens. Such a reduced nitrogen should be clearly apparent in the N$_{1s}$ X-ray photoelectron spectrum (XPS). The N$_{1s}$ high-resolution XP spectra for [PPN][Al(dpt)$_3$] (**4**) contains two distinct peaks. The larger peak at 395.21 eV is due to the PPN cation and the unreduced triazenide ligand whose assignment was confirmed by comparison with [PPN]Cl and Al(dpt)$_3$, while the smaller

(25) ^{1}H NMR for Al(dpt)$_3$ (THF-d_8) δ: 7.40 (4H, d, J(HH) = 7.6 Hz, *o*-C*H*), 7.20 (4H, t, J(HH) = 7.9 Hz, *m*-C*H*), 7.05 (2H, t, J(HH) = 7.9 Hz, *p*-C*H*).

(26) *NMR of Paramagnetic Molecules*; La Mar, G. N., Horrocks, W. D., Jr., Holm, R. H., Eds.; Academic Press: New York, 1973.

(27) (a) DeArmond, M. K.; Carlin, C. M. *Coord. Chem. Rev.* **1981**, *36*, 325. (b) Motten, A. G.; Hanck, K. W.; DeArmond, M. K. *Chem. Phys. Lett.* **1981**, *79*, 541.

(28) Giles, J. R. M.; Roberts, B. P. *J. Chem. Soc., Chem. Commun.* **1981**, 1167.

(29) Farrar, C. T.; Leman, J. T.; Larsen, S. C.; Braddock-Wilking, J.; Singel, D. J.; Barron, A. R. *J. Am. Chem. Soc.* **1995**, *117*, 1746.

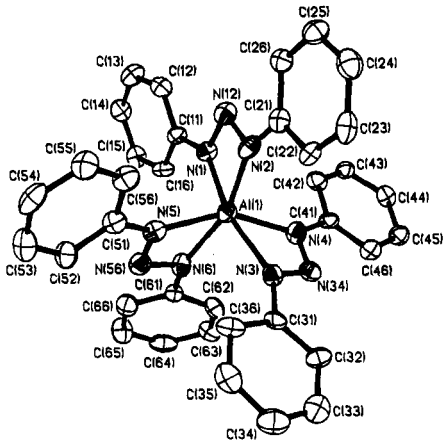

Figure 6. Structure of the $[Al(dpt)_3]^-$ anion in $[PPN][Al(dpt)_3]\cdot 5(THF)$ (**4**). Thermal ellipsoids are given at the 40% level, and all hydrogen atoms are omitted for clarity.

Table 2. Selected Bond Lengths (Å) and Bond Angles (deg) in $[PPN][Al(dpt)_3]\cdot 5(THF)$ (**4**)

Al(1)−N(1)	1.93(1)	Al(1)−N(2)	1.93(1)
Al(1)−N(3)	2.10(1)	Al(1)−N(4)	2.04(1)
Al(1)−N(5)	2.02(6)	Al(1)−N(6)	2.02(1)
N(1)−N(12)	1.41(1)	N(2)−N(12)	1.41(1)
N(3)−N(34)	1.33(2)	N(4)−N(34)	1.31(2)
N(5)−N(56)	1.31(2)	N(6)−N(56)	1.32(2)
N(1)−Al(1)−N(2)	67.7(4)	N(1)−Al(1)−N(3)	163.7(5)
N(1)−Al(1)−N(4)	103.6(5)	N(1)−Al(1)−N(5)	100.3(4)
N(1)−Al(1)−N(6)	100.7(4)	N(2)−Al(1)−N(3)	105.5(4)
N(2)−Al(1)−N(4)	99.5(5)	N(2)−Al(1)−N(5)	103.8(5)
N(2)−Al(1)−N(6)	160.8(5)	N(3)−Al(1)−N(4)	62.0(5)
N(3)−Al(1)−N(5)	95.7(4)	N(3)−Al(1)−N(6)	89.5(4)
N(4)−Al(1)−N(5)	151.5(5)	N(4)−Al(1)−N(6)	98.1(5)
N(5)−Al(1)−N(6)	62.1(4)	Al(1)−N(1)−N(12)	96.2(7)
Al(1)−N(2)−N(12)	96.4(7)	Al(1)−N(3)−N(34)	93.4(8)
Al(1)−N(4)−N(34)	96.9(8)	Al(1)−N(5)−N(56)	96.7(8)
Al(1)−N(6)−N(56)	96.2(8)	N(1)−N(12)−N(2)	99.4(8)
N(3)−N(34)−N(4)	108(1)	N(5)−N(56)−N(6)	105(1)

peak at a higher binding energy (398.98 eV) is consistent with a nitrogen in a reduced environment.[30]

Additional corroboration of the ligand-centered nature of the radical in the $[Al(dpt)_3]^{n-}$ anions is provided by a study of the electrochemistry and EPR of the gallium triazenide compound, $Ga(dpt)_3$. The cyclic voltammogram and differential pulse polarogram for $M(dpt)_3$ (M = Al and Ga) are essentially superimposable. Furthermore, the EPR spectrum of $[Ga(dpt)_3]^-$ shows no evidence for hyperfine coupling to the ^{69}Ga and ^{71}Ga (both $I = {}^3/_2$) nuclei.

X-ray Structural Determination of $[PPN][Al(dpt)_3]\cdot 5(THF)$. Supporting evidence for electron localization of the monoanionic complex is provided in the solid state by the X-ray crystallographic structural determination of the PPN salt of the monoreduced species, $[PPN][Al(dpt)_3]$ (**4**).

Dark red-black X-ray quality crystals of $(4)\cdot 5(THF)$ were obtained from a concentrated THF solution at −24 °C. The structure of the $[Al(dpt)_3]^-$ anion is shown in Figure 6; selected bond lengths and angles are given in Table 2. The X-ray crystal structure of this complex revealed two equivalent and one inequivalent triazene ligands. The unique triazenido ligand shows a lengthening in the N(1)−N(12) and N(2)−N(12) bond distances [average = 1.41 Å] and a concomitant decrease in the N(1)−N(12)−N(2) bond angle [99.4(8)°] (see Figure 7a) as compared to the two equivalent triazenides ($N-N_{av}$ = 1.32 Å, $N-N-N_{av}$ = 106.5°) and those in the unreduced complex $Al(dpt)_3$, which we have previously characterized by X-ray crystallography.[10] These distortions are as expected from the population of the N_3 π^* orbital upon reduction of a triazenide ligand. In fact, the changes in geometric parameters between the unique and the two equivalent triazenide ligands in $[Al(dpt)_3]^-$ are consistent with those predicted from *ab initio* calculations (see below). However, the magnitude of the increase in the observed N−N distance upon reduction [Δ(N−N) = 0.09(1) Å] is not as large as that calculated [Δ(N−N) = 0.104 Å]. Assuming the *ab initio* calculated distances are realistic, this difference may be accounted for by some partial delocalization of the unpaired electron onto the other triazenide ligands. Such a proposition is not unreasonable given the possibility of X-ray crystallographic disorder (see Experimental Section).

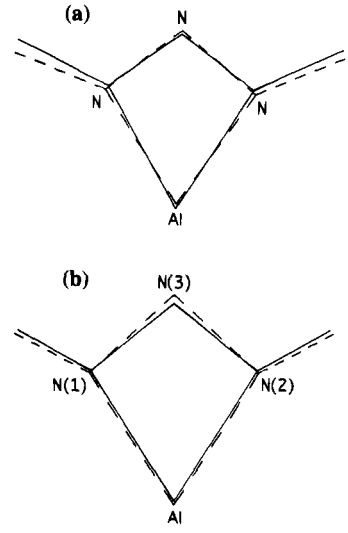

Figure 7. Overlay plots of a reduced (- - -) *vs* unreduced (—) triazenide ligand from (a) the crystallographic structural determination of $[PPN][Al(dpt)_3]$ (**2.4**) and (b) *ab inito* calculations of $Al(HNNNH)_3$ and $[Al(HNNNH)_3]^{3-}$.

From a consideration of the crystal packing diagram of $[PPN][Al(dpt)_3]\cdot 5(THF)$, it can clearly be seen that the anions and cations are closely packed in a pseudo fcc lattice. In spite of this, the size of the PPN cation dictates that the anions be clearly separated (Al···Al = 12.22 Å), in agreement with the EPR results. The closest cation−anion contact is between the central nitrogen of the unique (reduced) triazenide ligand and the *meta*-proton of one of the phenyl rings on the PPN cation. However, the distance [H(13D)···N(12) = 2.614 Å] is significantly larger than expected for a more normal hydrogen-bonded interaction (1.99−2.0 Å),[31] and it is more consistent with the dipole−dipole type interaction observed between an unreduced triazenide ligand and an indium−chlorine bond.[32]

Reduction of Substituted Triazenide Compounds: $Al(dpt\text{-}4\text{-}X)_3$ and $AlX_n(dpt)_{3-n}$. The availability of a range of substituted tris(1,3-diaryltriazenido) complexes, as well as alkyl and aryloxide derivatives,[31] allows for an investigation of changes in the reduction potentials of the complexes as a function of the triazenide ligand substituents, the change in the coordination number, and the introduction of other ligands into the aluminum coordination sphere. Electrochemical data for tris-triazenido complexes derived from substituted triazenes and

(30) Briggs, D.; Rivière, J. C. In *Practical Surface Analysis*; Briggs, D., Seah, M. P., Eds.; Wiley: New York, 1992; Chapter 3, p 122.

(31) Leman, J. T.; Braddock-Wilking, J.; Coolong, A. J.; Barron, A. R. *Inorg. Chem.* **1993**, *32*, 2986.

(32) Leman, J. T.; Roman, H. A.; Barron, A. R. *J. Chem. Soc., Dalton Trans.* **1992**, 2183.

Table 3. Electrochemical Data for Aluminum Triazenide Compounds[a]

compound	E_{pc} (V)	compound	E_{pc} (V)
Al(dpt-4-F)$_3$[b]	−1.50	Al(^{t}Bu)$_2$(dpt)	−1.90
Al(dpt-4-Cl)$_3$[b]	−1.64	Al(BHT)$_2$(dpt)	−2.00
Al(dpt-4-Br)$_3$[b]	−1.72	Al(^{t}Bu)(dpt)$_2$	−2.07
Al(dpt-F$_{10}$)$_3$[c]	−1.63	Al(BHT)(dpt)$_2$	−2.07
Al(^{t}Bu)$_2$(dpt)	−2.05		

[a] $E_{1/2} = (E_{pa} + E_{pc})/2$; $\Delta E_p = (E_{pa} - E_{pc})$. [b] dpt-4-X = 1,3-bis(4-X-phenyl)triazenide. [c] dpt-F$_{10}$ = 1,3-bis(pentafluorophenyl)triazenide.

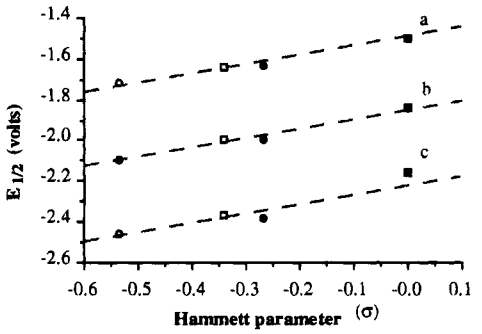

Figure 8. Plot of the first (a), second (b), and third (c) half-wave potentials for aluminum tris-triazenide compounds *vs* the Hämmett substituent constant (σ): (○) Al(dpt-4-OMe)$_3$, (□) Al(dpt-4-Me)$_3$, (●) Al(dpt*)$_3$, and (■) Al(dpt)$_3$.

alkyl and aryloxide aluminum triazenide compounds are given in Tables 1 and 3.

The tris-triazenido compounds fall into two categories: those exhibiting three quasireversible reduction waves (Table 1) and those with a single irreversible reduction wave (Table 3). The latter all have electron-withdrawing substituents on the triazenide's phenyl rings. We are uncertain as to the fate of the reduced species, and given the lack of correlation between reduction potential and electronegativity for the *p*-halo compounds, we view the substituents to be noninnocent.

In contrast, the tris-triazenido compounds with electron-donating substituents exhibit electrochemical behavior that mirrors the parent compound, Al(dpt)$_3$, as is shown in Table 1. ΔE_p values for these compounds bracket that found for the ferrocene/ferrocenium couple under the same conditions. The I_{pa}/I_{pc} values are comparable to those for Al(dpt)$_3$, with slightly limited chemical reversibility. The same difficulty in calculating the peak anodic/cathodic ratios is present here; however, when the potential is scanned only as far as the first wave, the ratio I_{pa}/I_{pc} can be determined precisely and exceeds 0.90 for all compounds.

We further note that the first, second, and third reduction potentials show a linear correlation (Figure 8) with the Hammett substituent constant (σ),[33] further corroborating the proposal of the ligand-based nature of the redox process in these systems. In addition, the reduction potentials are related to the longest wavelength transition in the UV−visible spectra (see Table 4 and Figure 9) such that molecules with the lowest wavelength (*i.e.*, those with the higher energy $\pi \rightarrow \pi^*$ transition) are the easiest to reduce.

The electron-donor-substituted compounds differ from Al(dpt)$_3$ in that three additional irreversible oxidation waves appear in the range −1.00 to +0.02 V upon the return oxidation scan. These waves do not appear unless the potential is scanned negative with respect to the first reduction wave, and they increase in intensity (maximally less than 30% of I_{pc}) as more scans are run. These observations indicate that these features are due to the oxidation of new species formed *after* the reduction processes occur, and will not be discussed further.

In a molecule containing multiple redox centers, the appearance of the cyclic voltammogram and the difference in half-wave potentials between successive reductions [$\Delta E_{1/2} = E_{1/2}^{n+1} - E_{1/2}^{n}$ (n = 1, 2, 3, ...)] are useful in ascertaining the degree of interaction between the reduced centers. For a tris-triazenido aluminum complex of interest here, in the limit of three redox-equivalent, completely noninteracting centers, values of $\Delta E_{1/2}$ = −36 mV (n = 1) and $\Delta E_{1/2}$ = −20 mV (n = 2) are predicted.[34] These values are sufficiently small that the corresponding waves would not be resolved, and a single three-electron wave should be observed. The resolution of three reduction waves for the tris-triazenido aluminum compounds therefore demonstrates that the redox events occur sequentially and at distinct potentials. It is worthy to note that for each individual compound, $\Delta E_{1/2}$ between the first and second and second and third reduction waves exceeds the predicted "no interaction" value and is the same within experimental error (see Table 1). While this indicates that the addition of each electron is not facilitated by the previous reduction step (*i.e.*, $\Delta E_{1/2} < 0$), the lack of variation for $\Delta E_{1/2}$ shows that the perturbation of the molecule is equal between each redox step. Further, there is little variation between $\Delta E_{1/2}$ values for Al(dpt)$_3$ and the three electron-rich complexes, which fall within the narrow range −320 to −380 mV. Together these results demonstrate that the tris-chelate structure is retained during reduction and are indicative of the common nature of the redox process for the compounds under consideration.

Cyclic voltammetry measurements of the alkyl and aryloxide aluminum triazenide compounds show a single irreversible reduction (see Table 3). Although no products could be isolated from chemical reductions, we note the following:

(a) No difference is observed between the reduction potentials of the isobutyl and *tert*-butyl or phenoxy homologues, thus indicating not only that the resulting radical is centered on the triazenide, but also that the nature of the ancillary ligands on aluminum (^{t}Bu *vs* ^{i}Bu *vs* BHT) does not affect the relative energy of the triazenide π^* orbital.

(b) There is a small increase in the reduction potential for Al(X)(dpt)$_2$ *vs* Al(X)$_2$(dpt), suggesting the coordination number of the aluminum does have a small effect on the reduction potential of the coordinated triazenide. It should be noted, however, that the effect of the coordination number (*ca.* 70 mV) is smaller than the ligand substitution effects (100−150 mV).

(c) The reduction of the aryloxide derivative does not result in the liberation of the BHT radical since upon repetitive cycling, the oxidation wave associated with this species (−0.35 V *vs* SCE) is not observed.

Theoretical Studies. In order to gain further understanding of the nature of the ligand orbitals populated during the formation of the radical anions, [Al(dpt)$_3$]$^{n-}$ (n = 1, 2, and 3), as well as the trends in the accompanying structural changes as a result of their population, we have carried out *ab initio* calculations on the model complex Al(HNNNH)$_3$ and its corresponding triply reduced form; calculated structural and geometrical data are given in Table 5.

The calculated distances and angles for Al(HNNNH)$_3$ are close to those determined experimentally for Al(dpt)$_3$ as well as its substituted triazenide derivatives. The N−N distance calculated for Al(HNNNH)$_3$ is within the range observed from

(33) McDaniel, D. H.; Brown, H. C. *J. Org. Chem.* **1958**, *23*, 420.

(34) Flanagan, J. B.; Margel, S.; Bard, A. J.; Anson, F. C. *J. Am. Chem. Soc.* **1978**, *100*, 4248.

Table 4. UV−Visible Spectroscopic Data for Aluminum Triazenide Compounds

compound	λ_1 (nm)	ϵ ($\times 10^4$) (L mol^{-1} cm^{-1})	λ_2 (nm)	ϵ ($\times 10^4$) (L mol^{-1} cm^{-1})	λ_3 (nm)	ϵ ($\times 10^4$) (L mol^{-1} cm^{-1})
Al(dpt)$_3$	238	4.6	294	2.9	354	6.5
Al(dpt-4-Me)$_3$[a]	240	4.5	296	2.6	360	6.1
Al(dpt-4-OMe)$_3$[a]	242	4.2	305	5.4	370	8.9
Al(dpt*)$_3$[b]	238	4.0	296	2.8	362	5.9
Al(dpt-4-F)$_3$[a]	218	2.7	294[d]	1.5	404	4.1
			338	4.0		
Al(dpt-4-Cl)$_3$[a]	244	2.7	342	3.9	419	6.0
Al(dpt-4-Br)$_3$[a]	242	4.0	306[d]	2.4	422	4.6
			368	6.0		
Al(dpt-F$_{10}$)$_3$[c]	238	2.7	*e*		370	7.3
Al(^{i}Bu)$_2$(dpt)	238	1.7	294	0.73	354	2.0
Al(^{t}Bu)$_2$(dpt)	236	2.3	294	0.82	356	2.2
Al(BHT)$_2$(dpt)	236	2.1	286	1.8	354	2.0
Al(^{i}Bu)(dpt)$_2$	238	3.0	294	1.4	354	3.5
Al(BHT)(dpt)$_2$	238	3.1	288	1.7	354	4.0

[a] dpt-4-X = 1,3-bis(4-X-phenyl)triazenide. [b] dpt* = 1-(*p*-methoxyphenyl)-3-phenyltriazenide. [c] dpt-F$_{10}$ = 1,3-bis(pentafluorophenyl)triazenide. [d] Shoulder on adjacent peak. [e] No separate band distinguishable.

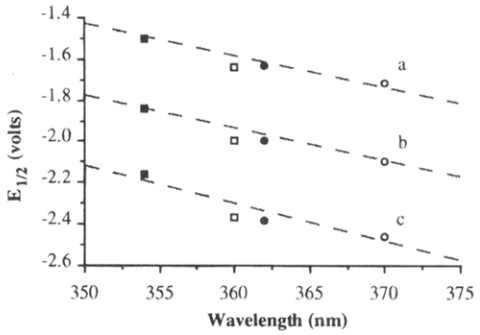

Figure 9. Plot of the first (a), second (b), and third (c) half-wave potentials for aluminum tris-triazenide compounds *vs* the N_3 $\pi \rightarrow \pi^*$ transition in the UV−visible spectrum: (○) Al(dpt-4-OMe)$_3$, (□) Al(dpt-4-Me)$_3$, (●) Al(dpt*)$_3$, and (■) Al(dpt)$_3$.

Table 5. STO-3G Structural Parameters for Al(HNNNH)$_3$ and [Al(HNNNH)$_3$]$^{3-}$ in Comparison with Experimental Values

molecule	parameter[a,b] (STO-3G)	calculated	experimental[c,d]
Al(HNNNH)$_3$	Al−N	1.917	1.968(4)−2.003(9)
	N−N	1.329	1.30(1)−1.33(1)
	N−Al−N$_{ch}$	65.3	63.7(3)−64.5(4)
	N−Al−N$_c$	99.8	90.8(4)−99.3(3)
	N−Al−N$_t$	157.9	153.8(2)−163.2(4)
	Al−N−N	96.2	93.9(6)−95.7(3)
	N−N−N	102.3	105.1(9)−106.5(8)
[Al(HNNNH)$_3$]$^{3-}$	Al−N	1.944	1.93(1)
	N−N	1.433	1.41(1)
	N−Al−N$_{ch}$	65.5	67.7(4)
	N−Al−N$_c$	98.5	*e*
	N−Al−N$_t$	155.4	*e*
	Al−N−N	100.0	96.2(7)−96.4(7)
	N−N−N	94.5	99.4(8)

[a] Bond distances in angstroms, angles in degrees. [b] N−Al−N: ch = chelate, c = cis, and t = trans. [c] In comparison with tris(diaryltriazenido)aluminum compounds, refs 12 and 31. [d] In comparison with the reduced ligand in [PPN][Al(dpt)$_3$], this work. [e] No direct comparison available.

X-ray crystallographic studies, while the calculated Al−N distance and N−N−N, Al−N−N, and N−Al−N angles show slight variations but are within experimental error of those determined by X-ray crystallography. Given the difference in steric effects between H and Ph, the level of the basis set (STO-3G), and the large estimated standard deviations of some of the experimental parameters, we do not attach any particular significance to these discrepancies and we believe the calculation faithfully reproduces the structural features of Al(dpt)$_3$.

Structural changes associated with ligand reduction may be predicted by comparison of calculated structural and geometrical parameters in the radical complex, [Al(HNNNH)$_3$]$^{3-}$, with those of the neutral complex, Al(HNNNH)$_3$ (see Table 5). For example, the N−N distance and the N−Al−N angle are increased upon reduction. In contrast, the N−N−N angle decreases upon ligand reduction. These changes may be clearly seen in Figure 7b and are in the direction expected from the population of the N_3 π^* orbital of the triazenide ligand, as well as those observed in the structural determination of compound **4** (see above).

The LUMO's calculated for Al(HNNNH)$_3$ are a set of three degenerate molecular orbitals, centered on the triazenide's N_3 unit, and are π^* in character (**II**). Assuming that no large

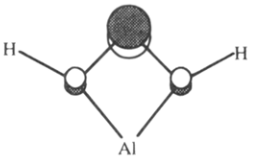

(**II**)

structural perturbations occur upon reduction, it is these orbitals that should be the sites for reduction in the neutral species and should thus become the singly occupied molecular orbitals (SOMO's) in the resulting anions. This is indeed found to be the case, as shown by the identity of the three degenerate SOMO's for the radical anion [Al(HNNNH)$_3$]$^{3-}$. From a consideration of the atomic orbital coefficients of the singly occupied molecular orbitals in the radical anion, the electron density of the unpaired electrons should be centered primarily on the central nitrogen of the N_3 unit. These results are, therefore, supportive of the EPR data that indicate that the unpaired electron of the radical species is localized on a single (central) nitrogen of the triazenide N_3 unit.

Conclusion

We have demonstrated for the first time that a homologous series of radical anionic aluminum complexes may be prepared, [Al(dpt)$_3$]$^{n-}$ (n = 1, 2, and 3), by either the electrochemical or the chemical reduction of Al(dpt)$_3$. On the basis of the spectroscopic characterization of the anionic complexes and *ab initio* calculations of the model system [Al(HNNNH)$_3$]$^{n-}$ (n = 0 and 3), we propose that the unpaired electron(s) is(are) ligand-centered in the triazenide's π^* orbital and localized on the central nitrogen of the N_3 unit. As a consequence of the partial

occupancy of the triazenide π^* orbital, there is a significant lowering of this orbital's energy and a change in the geometrical parameters of the AlN_3 cycle. These phenomena are predicted from *ab initio* calculations and confirmed by UV−visible spectroscopy and X-ray crystallographic data, respectively.

Substitution of the triazenide's phenyl rings has a large effect on the reduction potential of the coordinated triazenide and the stability of the resulting radical. Triazenide complexes substituted with electron donors are more difficult to reduce than the parent dpt complex, and as a consequence, the resulting anionic complexes are more reactive. Upon reduction of triazenide complexes with electron-withdrawing substituents, the resulting anions are unstable, as are complexes with alkyl or aryloxide ligands. The identity of the ancillary ligands was found to have no effect on the reduction potential of a coordinated triazenide; however, a small change was observed for changes in the aluminum coordination number.

Experimental Section

All manipulations were carried out under either prepurified nitrogen or argon. THF was distilled from sodium−benzophenone ketyl solution immediately before use and further degassed by three freeze−pump−thaw cycles. $Al(dpt)_3$ and substituted triazenide compounds were prepared as previously described.[10,28,31] All spectroscopic samples were prepared in a standard inert-atmosphere drybox equipped with a recirculating gas purifier.

Electrochemical experiments were performed with a combination PAR Model 174A polarographic analyzer/175 Universal programmer apparatus or a PAR Model 263 potentiostat/galvanostat at room temperature under an atmosphere of N_2. Measurements were made on 1×10^{-3} M solutions in THF with a conventional three-electrode setup (Pt disk working electrode (area = 0.2 cm^2), Pt gauze counter electrode, and a saturated aqueous calomel reference electrode) employing 0.1 M $[^nBu_4N][PF_6]$ as the supporting electrolyte. The reference and counter electrodes were each separated from the bulk analyte by a porous Teflon membrane sealed at the end of a salt bridge filled with the same electrolyte solution as in the main cell. The potential of the ferrocene/ferrocenium couple in this apparatus was 0.55 V, with $\Delta E_p = (E_{p_a} - E_{p_c}) = 180$ mV. I_{p_a}/I_{p_c} ratios were calculated by measuring peak currents relative to a base line extrapolated from the decaying current of the adjacent voltammetric peak or by the empirical method of Nicholson.[35] The I_{pa}/I_{pc} for the first reduction wave was determined, for all compounds, by scanning only the first reduction (without the subsequent waves) and then measuring directly. All reported potentials were measured at scan rates of 100 mV s^{-1} unless otherwise noted. The EPR spectra were recorded on approximately $(1-3) \times 10^{-3}$ M THF solutions in flame-sealed quartz tubes with a Varian E-109 spectrometer. The spectrometer was interfaced to an IBM PC computer for data storage. Low-temperature measurements at 77 K were achieved with the use of a commercially available finger dewar insert or a nitrogen gas flow cryostat designed for the Varian cavity. ^1H and ^{27}Al NMR spectra were obtained on Bruker AM-500 and WM-300 spectrometers, respectively, and chemical shifts are reported relative to the residual proton in THF-d_8 (7.15 ppm) (^1H) and $[Al(H_2O)_6]^{3+}$(^{27}Al). All spectra were recorded at room temperature in THF-d_8. UV−visible spectra were obtained in THF on a Hewlett-Packard 8452A diode array spectrophotometer as approximately 1×10^{-5} M solutions. Conductivity measurements were determined on approximately 1×10^{-3} M solutions with an A. H. Thomas Co. Serfas AC conductivity bridge RCM 15B1 using a cathode-ray oscillograph as a null detector. A dip-type cell with platinized electrodes (cell constant = 1.06 cm^{-1}) was calibrated with an aqueous KCl solution. Due to the difficulties of determining conductivity in nonpolarizing solvents such as THF, conductivities of multiple samples were measured at different concentrations $[(1-9) \times 10^{-3}$ M]. Values given are for the highest and lowest value obtained for each compound. X-ray photoelectron spectroscopy was carried out using a Surface Science SSX-100 spectrometer with Al-K_α monochromatized radiation.

(35) Nicholson, R. S. *Anal. Chem.* **1966**, *38*, 1406.

Elemental analyses were performed by Oneida Research Services, Inc., Whitesboro, NY. Significant variation in the C, H, and N analyses was observed for samples of compounds **1**, **2**, and **3a** due to variable amounts of THF in the samples. Analyses were therefore performed on a number of samples, and a range is given for each compound. The calculated values are based on the ideal formula $[Na(THF)_4]_n[Al(dpt)_3]$, where n is the charge on the aluminum anion. It should be noted that in each case the analysis is consistent with a general formula of $[Na(THF)_{4-\delta}]_n[Al(dpt)_3]$, where $0 < \delta < 2$. The Al:Na atomic ratios in compounds **1**, **2**, and **3a** were determined by XPS analysis of the oxidized residue of samples. This method provides an accurate value for the Al:Na ratio because any decomposition of the compounds yields nonvolatile aluminum and sodium species; the Na:Al ratio may be determined despite any decomposition that occurs in sample preparation.

$[Na(THF)_x]_n[Al(dpt)_3]$, n = 1 (1), 2 (2), and 3 (3). In a 100 mL Schlenk flask were placed $Al(dpt)_3$ (1.0 g, 1.6 mmol) and the appropriate molar equivalent[36] (plus *ca.* 5−10% excess) of sodium metal cut into small pieces. THF (50 mL) was added, and within 5 min the solution turned from bright orange to an intense dark red. The solution was stirred overnight at room temperature under argon and then filtered through Celite. The solvent was removed under vacuum to yield $[Na(THF)_4]_n[Al(dpt)_3]$ in approximately 75% isolated yield. The reduction of $Al(dpt)_3$ may also be accomplished with Li metal, Na/Hg amalgam, and sodium naphthalenide.

(1) Anal. Calcd for $[Na(THF)_4][Al(dpt)_3]$, $C_{52}H_{62}AlN_9NaO_4$: C, 67.38; H, 6.69; N, 13.60. Found: C, 67.41−67.60; H, 6.02−6.70; N, 13.70−15.23. Na:Al elemental ratio: 0.9 (calcd: 1.0). NMR (THF-d_8, δ): ^1H, 7.27 [4H, br s, *o*-C*H*], 7.04 [4H, br s, *m*-C*H*], 6.65 (2H, br s, *p*-C*H*]. Conductivity (concn): $\Lambda_M = 6.7$ (1.01×10^{-3} M), 6.9 (1.22×10^{-3} M) Ω^{-1} cm^2 mol^{-1}. UV−vis (λ, 2.2×10^{-5} M, THF): 240 ($\epsilon = 4.5 \times 10^4$ L mol^{-1} cm^{-1}), 294 ($\epsilon = 2.7 \times 10^4$ L mol^{-1} cm^{-1}), 358 ($\epsilon = 5.1 \times 10^4$ L mol^{-1} cm^{-1}), 410 ($\epsilon = 1.4 \times 10^4$ L mol^{-1} cm^{-1}), 520 ($\epsilon < 500$ L mol^{-1} cm^{-1}).

(2) Anal. Calcd for $[Na(THF)_4]_2[Al(dpt)_3]$, $C_{68}H_{94}AlN_9Na_2O_8$: C, 65.96; H, 7.59; N, 10.18. Found: C, 65.43−66.00; H, 5.94−7.32; N, 11.22−15.37. Na:Al elemental ratio: 1.8 (calcd: 2.0). NMR (THF-d_8, δ): ^1H, 7.27 [4H, br s, *o*-C*H*], 7.04 [4H, br s, *m*-C*H*], 6.64 [2H, br s, *p*-C*H*]. Conductivity (concn): $\Lambda_M = 9.7$ (9.53×10^{-3} M), 11.0 (1.78×10^{-3} M) Ω^{-1} cm^2 mol^{-1}. UV−vis (λ, 1.6×10^{-5} M, THF): 240 ($\epsilon = 4.8 \times 10^4$ L mol^{-1} cm^{-1}), 294 (shoulder), 360 ($\epsilon = 2.1 \times 10^4$ L mol^{-1} cm^{-1}), 410 ($\epsilon = 2.0 \times 10^4$ L mol^{-1} cm^{-1}), 524 ($\epsilon = 1.1 \times 10^4$ L mol^{-1} cm^{-1}).

(3) Anal. Calcd for $[Na(THF)_4]_3[Al(dpt)_3]$, $C_{84}H_{126}AlN_9Na_3O_{12}$: C, 65.11; H, 8.14; N, 8.14. Found: C, 64.82−65.00; H, 6.76−7.99; N, 9.13−9.46. Na:Al elemental ratio: 2.8 (calcd: 3.0). NMR (THF-d_8, δ): ^1H, 7.28 [4H, d, J(H−H) = 8.1 Hz, *o*-C*H*], 7.04 [4H, t, J(H−H) = 7.9 Hz, *m*-C*H*], 6.65 [2H, t, J(H−H) = 7.8 Hz, *p*-C*H*]. Conductivity (concn): $\Lambda_M = 9.9$ (1.06×10^{-3} M), 21.3 (2.39×10^{-3} M) Ω^{-1} cm^2 mol^{-1}. UV−vis (λ, 2.9×10^{-5} M, THF): 242 ($\epsilon = 6.6 \times 10^4$ L mol^{-1} cm^{-1}), 290 ($\epsilon = 5.5 \times 10^4$ L mol^{-1} cm^{-1}), 412 ($\epsilon = 3.1 \times 10^4$ L mol^{-1} cm^{-1}), 520 ($\epsilon = 5.5 \times 10^4$ L mol^{-1} cm^{-1}).

Chemical Oxidation of $[Al(dpt)_3]^{n-}$. A THF solution of $[Al(dpt)_3]^{n-}$ was cooled to −78 °C, and dry oxygen was carefully introduced into the head space above the solution. Upon stirring, the deep red-purple color rapid changed to bright orange. After 5 min, the volatiles were removed under vacuum. The residue was extracted with MeCN, from which orange $Al(dpt)_3$ was recovered upon cooling.[10]

$[PPN][Al(dpt)_3]$ (4). A solution of $[Na(THF)_x][Al(dpt)_3]$ prepared as above from $Al(dpt)_3$ (4.12 g, 6.69 mmol) and Na (0.166 g, 7.22 mmol) was filtered and added to a slurry of [PPN]Cl (3.86 g, 6.72 mmol) in THF (50 mL). The reaction mixture was stirred overnight, and a fine white precipitate was removed by filtration. The volume of the filtrate was reduced under vacuum to approximately 15 mL and then cooled to −24 °C. Large black crystals formed over a period of several weeks and were isolated by removing the mother liquid *via* cannula. A few crystals for the X-ray structural determination were set aside, and the remaining material was dried under vacuum, giving

(36) In order to avoid the possibility of a mixture of reduced species, the smallest possible stoichiometric excess of sodium was used in the generation of the samples for spectroscopic purposes.

Table 6. Summary of X-ray Diffraction Data for [PPN][Al(dpt)$_3$]·5(THF) (**4**)

formula	$C_{92}H_{100}AlO_5P$
space group	monoclinic, $P2_1/c$
a (Å)	19.101(6)
b (Å)	16.178(9)
c (Å)	28.00(1)
β (deg)	90.83(6)
V (Å^3)	8654(23)
Z	2
D (calcd) (g/cm^3)	1.163
cryst dimens (mm)	0.33 × 0.35 × 0.39
temp (K)	298
radiation	Mo Kα (λ = 0.710 73 Å) graphite monochromater
μ (cm^{-1})	0.117
2θ limits	4.0−40.0
scan type	ω
no. of data collected	8729
no. of unique data	8004
no. of observed data	5380 ($F > 4.0\sigma F$)
weighting scheme	$\omega^{-1} = \sigma^2(\lvert F_o\rvert) + 0.0018(\lvert F_o\rvert)^2$
R	0.093
R_w	0.098
final residual (e Å^{-3})	1.67

4.87 g of product with approximate composition [PPN][Al(dpt)$_3$]·2(THF). Yield: 56%. Mp: > 180 °C dec. Anal. Calcd for $C_{80}H_{76}AlN_{10}O_2P$: C, 74.00; H, 5.90; N, 10.79. Found: C, 73.26; H, 5.83; N, 10.70.[37] NMR (THF, δ): ^{27}Al, 56 ($W_{1/2}$ = 7500 Hz).

[Na(THF)$_x$][Ga(dpt)$_3$]. This compound was prepared in a fashion analogous to that of the [Na(THF)$_x$]$_n$[Al(dpt)$_3$] compounds, using Ga(dpt)$_3$[10] (0.874 g, 1.33 mmol) and Na metal (0.032 g, 1.4 mmol) in THF (35 mL).

X-ray Crystallographic Studies. A crystal data summary is given in Table 6; fractional atomic coordinates are listed in Table 7.

In addition to being sensitive to oxygen, the crystals of **4**·5(THF) readily lost THF of solvation. Removal of the crystals from the mother liquor caused them to powder within seconds, even under an inert atmosphere. Attempts to cool the crystal below ambient temperatures to enhance the quality of the collected data resulted in the crystal cracking. The crystals were therefore sealed in a glass capillary along with a small quantity of the supernatant solution. Under these conditions, minimal deterioration of the crystal was observed during the data collection. However, the crystals were poorly diffracting, precluding data collection above 2θ = 40.0°.

Unit-cell parameters and intensity data were obtained by following previously detailed procedures,[38] using a Nicolet R3m/v diffractometer operating in the $\theta-2\theta$ scan mode.[39] Experimental data are given in Table 6. The structure was solved using the direct methods program XS, which revealed the position of most of the heavy atoms, the remainder of which were located using standard difference method techniques. All the hydrogen atoms were included as fixed atom contributors in the final cycles, d(C−H) = 0.96 Å and U(iso) = 0.08 Å^2.

Despite the location and refinement of all the non-hydrogen atoms, the R factor of 0.093 and the high estimated standard deviations for some bond distances and angles could not be further reduced. This may be due to a number of parameters: (a) the high thermal motion associated with the 298 K data collection and the "light atom" nature of the structure, (b) a loss of solvent from the crystal lattice, (c) oxidation of the radical to the neutral complex Al(dpt)$_3$, and (d) the possibility that like in transition metal bipy complexes, the unpaired electron in compound **4**, while primarily localized on one of the triazenides [N(1)−N(2)], is significantly disordered if observed over the other two triazenide ligands. However, since all the chemically equivalent structural parameters are within experimental error of each other and, most importantly, within the range of previously reported values and the structure is wholly consistent with the EPR and UV−visible spectroscopic data, this solution is chemically reasonable and undoubtedly correct.

Details of the refinement are given in Table 6. Atomic scattering factors and anomalous scattering parameters were as given in the literature.[40]

Computational Methods. *Ab initio* all electron molecular orbital (MO) calculations were performed on a Stardent computer using the GAUSSIAN 90[41] suite of programs. Optimized structures for Al(HNNNH)$_3$ and [Al(HNNNH)$_3$]$^{3-}$ were determined at the Hartree−Fock level with the STO-3G basis set.[42] A calculation at the UHF/3-21G* basis set level was subsequently executed using the optimized

Table 7. Selected[a] Atomic Coordinates (×10^4) and Equivalent Isotropic Displacement Coefficients (Å × 10^3)[b] for [PPN][Al(dpt)$_3$]·5(THF) (**4**)

	x	y	z	U(eq)
Al(1)	12 897(2)	9449(2)	1592(1)	42(1)
N(1)	12 325(5)	8702(6)	1954(3)	42(4)
N(12)	12 754(5)	8690(6)	2368(3)	54(4)
N(2)	13 264(5)	9271(6)	2227(4)	51(4)
N(3)	13 415(6)	10 497(7)	1338(4)	46(4)
N(34)	12 914(6)	11 013(7)	1477(4)	46(4)
N(4)	12 437(6)	10 572(7)	1685(4)	50(4)
N(5)	13 431(5)	8626(6)	1196(4)	44(4)
N(56)	13 007(6)	8640(7)	822(4)	53(5)
N(6)	12 540(6)	9212(7)	927(4)	46(4)
C(11)	11 773(6)	8126(8)	1922(5)	41(5)
C(12)	11 676(7)	7518(9)	2258(5)	49(5)
C(13)	11 131(7)	6945(9)	2206(6)	57(6)
C(14)	10 691(7)	6981(9)	1810(5)	55(6)
C(15)	10 760(6)	7606(9)	1475(5)	44(5)
C(16)	11 300(7)	8160(8)	1530(5)	47(5)
C(21)	13 758(6)	9472(8)	2575(5)	45(5)
C(22)	14 267(7)	10 083(8)	2469(5)	49(5)
C(23)	14 739(7)	10 322(9)	2810(6)	60(6)
C(24)	14 764(8)	9953(10)	3266(6)	67(7)
C(25)	14 262(7)	9340(9)	3371(5)	57(6)
C(26)	13 765(7)	9097(8)	3032(5)	49(5)
C(31)	13 948(7)	10 815(9)	1062(4)	40(5)
C(32)	13 983(7)	11 637(9)	956(5)	50(6)
C(33)	14 520(8)	11 898(10)	642(6)	67(6)
C(34)	14 994(8)	11 383(12)	457(6)	70(7)
C(35)	14 969(7)	10 548(11)	593(5)	63(6)
C(36)	14 448(7)	10 258(9)	898(5)	52(5)
C(41)	11 842(7)	10 980(8)	1886(4)	42(5)
C(42)	11 365(7)	10 525(9)	2139(5)	51(5)
C(43)	10 796(7)	10 898(8)	2339(4)	45(5)
C(44)	10 708(7)	11 753(9)	2292(5)	49(5)
C(45)	11 175(7)	12 211(9)	2034(5)	52(5)
C(46)	11 754(6)	11 831(9)	1816(5)	48(5)
C(51)	14 025(7)	8077(9)	1172(6)	51(6)
C(52)	14 197(7)	7691(9)	751(6)	56(6)
C(53)	14 775(8)	7176(9)	750(6)	68(7)
C(54)	15 161(7)	7039(9)	1167(7)	64(7)
C(55)	14 994(7)	7439(10)	1582(6)	62(6)
C(56)	14 416(7)	7961(9)	1586(6)	59(6)
C(61)	11 985(7)	9311(8)	581(5)	45(5)
C(62)	11 596(7)	10 024(9)	585(5)	53(6)
C(63)	11 056(7)	10 158(9)	271(5)	56(6)
C(64)	10 928(7)	9561(12)	−82(5)	66(6)
C(65)	11 301(8)	8833(10)	−105(5)	66(6)
C(66)	11 860(7)	8720(9)	238(5)	61(6)

[a] For atomic positions of the PPN cation and THF molecules, see supplementary material. [b] Equivalent isotropic U(eq) defined as one-third of the trace of the orthogonalized $\mathbf{U}_{ij}$ tensor.

(37) Difficulties with obtaining consistent elemental analysis are undoubtedly due to the presence of nonstoichiometric amounts of THF remaining even after vacuum drying of the crystals.

(38) Healy, M. D.; Wierda, D. A.; Barron, A. R. *Organometallics* **1988**, 7, 2543.

(39) *P3/R3 Data Collection Manual*; Nicolet Instrument Corp.: Madison, WI, 1987.

(40) *International Tables for X-ray Crystallography*; Kynoch Press: Birmingham, AL, 1974; Vol. 4.

(41) Frisch, M. J.; Head-Gordon, M.; Trucks, G. W.; Foresman, J. B.; Schlegel, H. B.; Raghavachari, K.; Robb, M.; Binkley, J. S.; Gonzalez, C.; DeFrees, D. J.; Fox, D. J.; Whiteside, R. A.; Seeger, R.; Melius, C. F.; Baker, J.; Martin, R. L.; Kahn, L. R.; Stewart, J. J. P.; Topiol, S.; Pople, J. A. *GAUSSIAN 90*, Revision H; Gaussian, Inc.: Pittsburgh, PA, 1990.

parameters. We have previously found the UHF/3-21G* model to give good descriptions of the structures of organoaluminum compounds.[43] In this work we are seeking not the prediction of absolute structures but rather a qualitative explanation for observed structural features. In this regard, including the limit of computer time, we do not feel the application of a larger basis set is warranted. To further reduce the size of the calculation, the phenyl rings of the triazene ligands were replaced by protons that were restrained to lie in the N_3 plane of each triazenide unit.

(42) First-row elements: Binkley, J. S.; Pople, J. A.; Hehre, W. J. *J. Am. Chem. Soc.* **1988**, *110*, 939. Second-row elements: Pietro, W. J.; Francl, M. M.; Hehre, W. J.; DeFrees, D. J.; Pople, J. A.; Binkley, J. S. *J. Am. Chem. Soc.* **1982**, *104*, 5039.

(43) Barron, A. R.; Dobbs, K. D.; Francl, M. M. *J. Am. Chem. Soc.* **1991**, *113*, 39 and references therein.

Acknowledgment. This work was funded by grants from the Aluminum Research Board. We are grateful to Richard Miller (Akzo Chemicals) for the gift of $AlMe_3$.

Supplementary Material Available: Full listings of bond length and angles, anisotropic thermal parameters, and hydrogen atom parameters (9 pages); tables of calculated and observed structure factors (29 pages). This material is contained in many libraries on microfiche, immediately follows this article in the microfilm version of the journal, and can be ordered from the ACS; see any current masthead page for ordering information.

JA940576M